

Asymptotic scaling properties of the posterior mean and variance in the Gaussian scale mixture model

Rodrigo Echeveste, Guillaume Hennequin, Máté Lengyel

Computational and Biological Learning Lab, Dept. of Engineering, University of Cambridge, Cambridge, UK

December 14, 2024

Contents

1	Introduction	1
2	Recap: definition of the GSM	2
2.1	The generative model	2
2.2	Posterior inference	2
3	Results	3
3.1	Inferring z	3
3.2	Low-dimensional posterior	3
3.3	Low and high contrast limit scaling for the mean and the variance	4
3.4	Numerical validation	6
4	Discussion	10
5	Methods	10
	Appendix	15
A	Deriving the low-dimensional posterior	15
B	Computing the inverse of $\left(\frac{z^2}{\sigma_x^2} \bar{\mathbf{R}}_o + \mathbf{I}\right)$ and its asymptotic form in the undercomplete case	15
C	Numerical evaluation of z_{MAP}	16
D	On the invertibility of $\bar{\mathbf{R}}_o$ and its rank	17

1 Introduction

The Gaussian scale mixture model (GSM) is a simple yet powerful probabilistic generative model of natural image patches (Wainwright and Simoncelli, 1999). In line with the well-established idea that sensory processing is adapted to the statistics of the natural environment (Fiser et al., 2010), the GSM has also been considered a model of the early visual system, as a reasonable “first-order” approximation to the internal model that the primary visual cortex (V1) inverts. According to this view, neural

activities in V1 represent the posterior distribution under the GSM given a particular visual stimulus. Indeed, (approximate) inference under the GSM has successfully accounted for various nonlinearities in the mean (trial-average) responses of V1 neurons (Schwartz and Simoncelli, 2001; Coen-Cagli et al., 2015), as well as the dependence of (across-trial) response variability with stimulus contrast found in V1 recordings (Orbán et al., 2016). However, previous work almost exclusively relied on numerical simulations to obtain these results. Thus, for a deeper insight into the realm of possible behaviours the GSM can (and cannot) exhibit and predict, here we present analytical derivations for the limiting behaviour of the mean and (co)variance of the GSM posterior at very low and high contrast levels. These results should guide future work exploring neural circuit dynamics appropriate for implementing inference under the GSM.

2 Recap: definition of the GSM

2.1 The generative model

According to the GSM, an image patch $\mathbf{x} \in \mathbb{R}^{N_x}$ is constructed by linearly combining a (fixed) set of local features, $\mathbf{A} \in \mathbb{R}^{N_x \times N_y}$, weighted by a set of (image-specific) coefficients, $\mathbf{y} \in \mathbb{R}^{N_y}$, and scaled by a single global (contrast) variable, $z \in \mathbb{R}$, plus additive white Gaussian noise:

$$\mathbf{x}|\mathbf{y}, z \sim \mathcal{N}(z \bar{\mathbf{x}}, \sigma_x^2 \mathbf{I}), \text{ with } \bar{\mathbf{x}} = \mathbf{A} \mathbf{y} \quad (1)$$

where the feature coefficients are drawn from a multivariate Gaussian distribution

$$\mathbf{y} \sim \mathcal{N}(\mathbf{0}, \mathbf{C}) \quad (2)$$

and the contrast, z , is drawn from a prior which we choose here to be a power-law:¹

$$\mathcal{P}(z) = \frac{(n-1) b^{n-1}}{(z+b)^n} \quad (3)$$

with $b > 0$ and $n > 1$. It is the global contrast variable, z , which allows the model to produce higher-order statistical dependencies between local features, which are typically present in natural images (Schwartz and Simoncelli, 2001).

2.2 Posterior inference

The posterior under the GSM for a given image, \mathbf{x} , can be written as

$$\mathcal{P}(\mathbf{y}|\mathbf{x}, z) = \mathcal{N}(\boldsymbol{\mu}, \boldsymbol{\Sigma}) \quad (4)$$

$$\text{with } \boldsymbol{\mu} = \frac{z}{\sigma_x^2} \boldsymbol{\Sigma} \mathbf{A}^\top \mathbf{x} \quad (5)$$

$$\text{and } \boldsymbol{\Sigma} = \left(\mathbf{C}^{-1} + \frac{z^2}{\sigma_x^2} \mathbf{A}^\top \mathbf{A} \right)^{-1} \quad (6)$$

In order to compute $\mathcal{P}(\mathbf{y}|\mathbf{x})$, the moments of which we are ultimately interested in (see above), we need to marginalise over z using $\mathcal{P}(z|\mathbf{x})$:

$$\mathcal{P}(\mathbf{y}|\mathbf{x}) = \int \mathcal{P}(\mathbf{y}|\mathbf{x}, z) \mathcal{P}(z|\mathbf{x}) dz \quad (7)$$

¹In results to be presented elsewhere, we show how other popular choices for the prior, such as a gamma distribution or a truncated Gaussian, while showing similar qualitative results within the range of interest for the contrast, present divergent behaviour in the limit of very high contrast.

3 Results

We seek to understand how the mean and (co)variance of the posterior over feature coefficients, $\mathcal{P}(\mathbf{y}|\mathbf{x})$, scale with contrast. In particular, we are interested in their asymptotic behaviour in the low- and high-contrast limits.

3.1 Inferring z

In the following, we distinguish between

z^* , the true contrast of an image, such that we assume that the image, \mathbf{x} , can be rewritten as a ‘base image’, $\bar{\mathbf{x}}$, scaled by this true contrast:²

$$\mathbf{x} = z^* \bar{\mathbf{x}} \quad (8)$$

z , the inferred contrast when that image is presented, i.e. the variable that needs to be inferred (and eventually marginalised out, see [Equation 7](#)) under the GSM;

z_{MAP} , the maximum *a posteriori* (MAP) estimate of the contrast, i.e. the setting of z that maximises its posterior for a given image: $z_{\text{MAP}} = \arg\max_z \mathcal{P}(z|\mathbf{x})$.

We study two levels of approximation. First, we assume $\mathcal{P}(z|\mathbf{x}) \simeq \delta(z - z_{\text{MAP}})$, and therefore $\mathcal{P}(\mathbf{y}|\mathbf{x}) \simeq \mathcal{P}(\mathbf{y}|\mathbf{x}, z = z_{\text{MAP}})$ (see [Equation 7](#)) which makes $\mathcal{P}(\mathbf{y}|\mathbf{x})$ a multivariate Gaussian ([Equation 4](#)). Second, we also consider a further approximation, by assuming that $z_{\text{MAP}} = z^*$, and thus $\mathcal{P}(\mathbf{y}|\mathbf{x}) \simeq \mathcal{P}(\mathbf{y}|\mathbf{x}, z = z^*)$, as in the limit of large images the contrast should be near-perfectly inferred. Thus, our strategy for analysing how the mean and (co)variance of $\mathcal{P}(\mathbf{y}|\mathbf{x})$ scale with z^* will proceed in two steps. We compute these quantities first as functions of z_{MAP} and then, via a mapping from z^* to z_{MAP} , as functions of z^* (either computing the z^* -to- z_{MAP} mapping numerically, or, taking the second approximation, simply assuming an identity mapping). For brevity, we present below ([Sections 3.2](#) to [3.3](#)) the analytical results for the second, cruder approximation only, $\mathcal{P}(\mathbf{y}|\mathbf{x}) \simeq \mathcal{P}(\mathbf{y}|\mathbf{x}, z = z^*)$, and refer the reader to the Methods ([Section 5](#)) for the analytical form of the first, milder approximation, $\mathcal{P}(\mathbf{y}|\mathbf{x}) \simeq \mathcal{P}(\mathbf{y}|\mathbf{x}, z = z_{\text{MAP}})$. We close this section by showing numerical results for both approximations ([Section 3.4](#)).

3.2 Low-dimensional posterior

As we are only interested in coarse summary statistics of the moments of the posterior (e.g. average mean and variance over all features, or mean/variance for a single feature), we express the posterior for a subset of the latent variables, which we call \mathbf{y}_\bullet , with the rest of the latent variables denoted by \mathbf{y}_\circ (such that $\mathbf{y} = \{\mathbf{y}_\bullet, \mathbf{y}_\circ\}$). We denote the corresponding columns of \mathbf{A} by \mathbf{A}_\bullet and \mathbf{A}_\circ , and the corresponding blocks of \mathbf{C} by $\mathbf{C}_\bullet = \text{Cov}[\mathbf{y}_\bullet]$, $\mathbf{C}_\circ = \text{Cov}[\mathbf{y}_\circ]$, and $\mathbf{C}_{\circ\bullet} = \text{Cov}[\mathbf{y}_\circ, \mathbf{y}_\bullet]$.

²Note that this is slightly inconsistent with the generative model ([Equation 1](#)), which assumes that observation noise gets added to the image after the scaling by contrast.

Thus, this low-dimensional posterior is (see [Appendix A](#) for a detailed derivation):

$$\mathbf{y}_\bullet | \mathbf{x}, z \sim \mathcal{N}(\boldsymbol{\mu}_\bullet, \boldsymbol{\Sigma}_\bullet) \quad (9)$$

$$\text{where } \boldsymbol{\mu}_\bullet = \frac{z}{\sigma_x^2} \boldsymbol{\Sigma}_\bullet \bar{\mathbf{A}}_\bullet^\top \left(\frac{z^2}{\sigma_x^2} \bar{\mathbf{R}}_\bullet + \mathbf{I} \right)^{-1} \mathbf{x} \quad (10)$$

$$\text{and } \boldsymbol{\Sigma}_\bullet = \left[\mathbf{C}_\bullet^{-1} + \frac{z^2}{\sigma_x^2} \bar{\mathbf{A}}_\bullet^\top \left(\frac{z^2}{\sigma_x^2} \bar{\mathbf{R}}_\bullet + \mathbf{I} \right)^{-1} \bar{\mathbf{A}}_\bullet \right]^{-1} \quad (11)$$

with

$$\bar{\mathbf{A}}_\bullet = \mathbf{A}_\bullet + \mathbf{A}_\circ \mathbf{C}_{\circ\bullet} \mathbf{C}_\bullet^{-1} \quad (12)$$

$$\bar{\mathbf{R}}_\bullet = \mathbf{A}_\circ (\mathbf{C}_\circ - \mathbf{C}_{\circ\bullet} \mathbf{C}_\bullet^{-1} \mathbf{C}_{\circ\bullet}^\top) \mathbf{A}_\circ^\top \quad (13)$$

(Note that [Equations 9-11](#) give back, as they should, [Equations 4-6](#) in the special case when all of \mathbf{y} is included in \mathbf{y}_\bullet , and so $\mathbf{A}_\circ = \mathbf{0}$ and thus $\bar{\mathbf{R}}_\bullet = \mathbf{0}$.)

3.3 Low and high contrast limit scaling for the mean and the variance

In what follows we present scaling laws for the mean and the variance of the GSM, as a function of the (true) contrast variable z^\star , both in the low contrast (LC) limit ($z^\star \rightarrow 0$) and in the high contrast (HC) limit ($z^\star \rightarrow \infty$). Up to second order in z^\star , these take the general form (see [Section 5](#), Methods, for the derivations):

Low contrast:

$$\boldsymbol{\mu}_\bullet^{\text{LC}}(z^\star) \simeq \boldsymbol{\mu}_\bullet^0 + \frac{z^{\star 2}}{\sigma_x^2} \mathbf{M}^{\text{LC}} \bar{\mathbf{x}} \quad (14)$$

$$\boldsymbol{\Sigma}_\bullet^{\text{LC}}(z^\star) \simeq \boldsymbol{\Sigma}_\bullet^0 - \frac{z^{\star 2}}{\sigma_x^2} \mathbf{V}^{\text{LC}} \quad (15)$$

High contrast:

$$\boldsymbol{\mu}_\bullet^{\text{HC}}(z^\star) \simeq \boldsymbol{\mu}_\bullet^\infty - \frac{\sigma_x^2}{z^{\star 2}} \mathbf{M}^{\text{HC}} \bar{\mathbf{x}} \quad (16)$$

$$\boldsymbol{\Sigma}_\bullet^{\text{HC}}(z^\star) \simeq \boldsymbol{\Sigma}_\bullet^\infty + \frac{\sigma_x^2}{z^{\star 2}} \mathbf{V}^{\text{HC}} \quad (17)$$

Where $\boldsymbol{\mu}_\bullet^0$, $\boldsymbol{\mu}_\bullet^\infty$, $\boldsymbol{\Sigma}_\bullet^0$, $\boldsymbol{\Sigma}_\bullet^\infty$, $\mathbf{M}^{\text{LC/HC}}$, $\mathbf{V}^{\text{LC/HC}}$ are constant vectors and matrices, independent of the contrast level z^\star , such that $\boldsymbol{\mu}_\bullet^0$, $\boldsymbol{\Sigma}_\bullet^0$, $\boldsymbol{\mu}_\bullet^\infty$, $\boldsymbol{\Sigma}_\bullet^\infty$ correspond to the asymptotic values of the mean and (co)variance at zero / infinite contrast, while $\mathbf{M}^{\text{LC/HC}}$ and $\mathbf{V}^{\text{LC/HC}}$ determine the speed of convergence towards these asymptotes. These equations reveal that in the low contrast regime, the magnitude of $\boldsymbol{\mu}_\bullet$ and $\boldsymbol{\Sigma}_\bullet$ grow quadratically. We also see that in the limit of infinite contrast, both the mean and variance decay towards their respective asymptotic values as $1/z^{\star 2}$.

In the low contrast limit, we find (see [Section 5](#) for details):

$$\boldsymbol{\mu}_\bullet^0 = \mathbf{0} \quad (18)$$

$$\mathbf{M}^{\text{LC}} = \mathbf{C}_\bullet \bar{\mathbf{A}}_\bullet^\top \quad (19)$$

$$\boldsymbol{\Sigma}_\bullet^0 = \mathbf{C}_\bullet \quad (20)$$

$$\mathbf{V}^{\text{LC}} = \mathbf{C}_\bullet \bar{\mathbf{A}}_\bullet^\top \bar{\mathbf{A}}_\bullet \mathbf{C}_\bullet \quad (21)$$

Thus, the magnitude of the mean will grow quadratically from 0 (which is the prior mean), while the variance (of a single unit) will decrease quadratically from the prior variance (because \mathbf{V}^{LC} is positive definite, and so in the scalar case, it is positive).

In the high contrast limit, the inverse of the matrix $\left(\frac{z^2}{\sigma_x^2} \bar{\mathbf{R}}_o + \mathbf{I}\right)^{-1}$, present both in [Equations 10](#) and [11](#), imposes some limitations when $\bar{\mathbf{R}}_o$ is itself not invertible. We note that for an overcomplete model (formally, in which $\text{rank}(\mathbf{A}_o) = N_x \leq N_{y_o}$), $\bar{\mathbf{R}}_o$ will be invertible. However, for an undercomplete model (which we will here restrict to the case $\text{rank}(\mathbf{A}_o) = N_{y_o} \leq N_x$), $\bar{\mathbf{R}}_o$ will be low rank and thus non-invertible, in which case we will make use of its Cholesky decomposition:

$$\bar{\mathbf{R}}_o = \mathbf{A}_o \mathbf{L}_o \mathbf{L}_o^T \mathbf{A}_o^T \quad (22)$$

where, in turn, \mathbf{L}_o is the Cholesky factor of $\mathbf{C}_o - \mathbf{C}_{o\bullet} \mathbf{C}_{\bullet\bullet}^{-1} \mathbf{C}_{o\bullet}^T$:

$$\mathbf{L}_o \mathbf{L}_o^T = \mathbf{C}_o - \mathbf{C}_{o\bullet} \mathbf{C}_{\bullet\bullet}^{-1} \mathbf{C}_{o\bullet}^T \quad (23)$$

With these considerations, we obtain separate solutions for the over- and undercomplete cases (see [Section 5](#) for details):³

Overcomplete system

$$\boldsymbol{\Sigma}_{\bullet}^{\infty} = \left(\mathbf{C}_{\bullet\bullet}^{-1} + \bar{\mathbf{A}}_{\bullet}^T \bar{\mathbf{R}}_o^{-1} \bar{\mathbf{A}}_{\bullet} \right)^{-1} \quad (24)$$

$$\mathbf{V}^{HC} = \boldsymbol{\Sigma}_{\bullet}^{\infty} \bar{\mathbf{A}}_{\bullet}^T \bar{\mathbf{R}}_o^{-1} \bar{\mathbf{R}}_o^{-1} \bar{\mathbf{A}}_{\bullet} \boldsymbol{\Sigma}_{\bullet}^{\infty} \quad (25)$$

$$\boldsymbol{\mu}_{\bullet}^{\infty} = \boldsymbol{\Sigma}_{\bullet}^{\infty} \bar{\mathbf{A}}_{\bullet}^T \bar{\mathbf{R}}_o^{-1} \bar{\mathbf{x}} \quad (26)$$

$$\mathbf{M}^{HC} = \boldsymbol{\Sigma}_{\bullet}^{\infty} \bar{\mathbf{A}}_{\bullet}^T \bar{\mathbf{R}}_o^{-1} \bar{\mathbf{R}}_o^{-1} \left(\mathbf{I} - \bar{\mathbf{A}}_{\bullet} \boldsymbol{\Sigma}_{\bullet}^{\infty} \bar{\mathbf{A}}_{\bullet}^T \bar{\mathbf{R}}_o^{-1} \right) \quad (27)$$

$$(28)$$

Undercomplete system

$$\boldsymbol{\Sigma}_{\bullet}^{\infty} = \mathbf{0} \quad (29)$$

$$\mathbf{V}^{HC} = \left(\bar{\mathbf{A}}_{\bullet}^T \mathbf{Q}_o^{\infty} \bar{\mathbf{A}}_{\bullet} \right)^{-1} \quad (30)$$

$$\boldsymbol{\mu}_{\bullet}^{\infty} = \mathbf{V}^{HC} \bar{\mathbf{A}}_{\bullet}^T \mathbf{Q}_o^{\infty} \bar{\mathbf{x}} \quad (31)$$

$$\mathbf{M}^{HC} = \mathbf{V}^{HC} \left[\left(\mathbf{C}_{\bullet\bullet}^{-1} + \bar{\mathbf{A}}_{\bullet}^T \mathbf{Q}_o^{\infty} \bar{\mathbf{A}}_{\bullet} \right) \mathbf{V}^{HC} \bar{\mathbf{A}}_{\bullet}^T \mathbf{Q}_o^{\infty} - \bar{\mathbf{A}}_{\bullet}^T \mathbf{Q}_o^{\infty} \right] \quad (32)$$

with

$$\mathbf{Q}_o^{\infty} = \mathbf{I} - \mathbf{A}_o \mathbf{L}_o \left(\mathbf{L}_o^T \mathbf{A}_o^T \mathbf{A}_o \mathbf{L}_o \right)^{-1} \mathbf{L}_o^T \mathbf{A}_o^T \quad (33)$$

$$\bar{\mathbf{Q}}_o = \mathbf{A}_o \mathbf{L}_o \left(\mathbf{L}_o^T \mathbf{A}_o^T \mathbf{A}_o \mathbf{L}_o \right)^{-2} \mathbf{L}_o^T \mathbf{A}_o^T \quad (34)$$

Note that the posterior variance only shrinks to zero in the undercomplete but not in the overcomplete case. This is because in the overcomplete case, the input is only able to pin down the value of the latent variables to a (linear) subspace, so the full posterior tends towards a rank-deficient (zero-thickness) ‘pancake’ which marginalises to a full-rank (finite-volume) ‘cloud’ when projected down to a low-dimensional subspace, thus leaving some ever-lingering uncertainty within that subspace. In contrast, in the undercomplete case, the input actually overconstrains the latents (bar the effect of observation noise), and so the posterior tends towards a Dirac delta function which remains a delta function even after projecting down to a low-dimensional subspace.

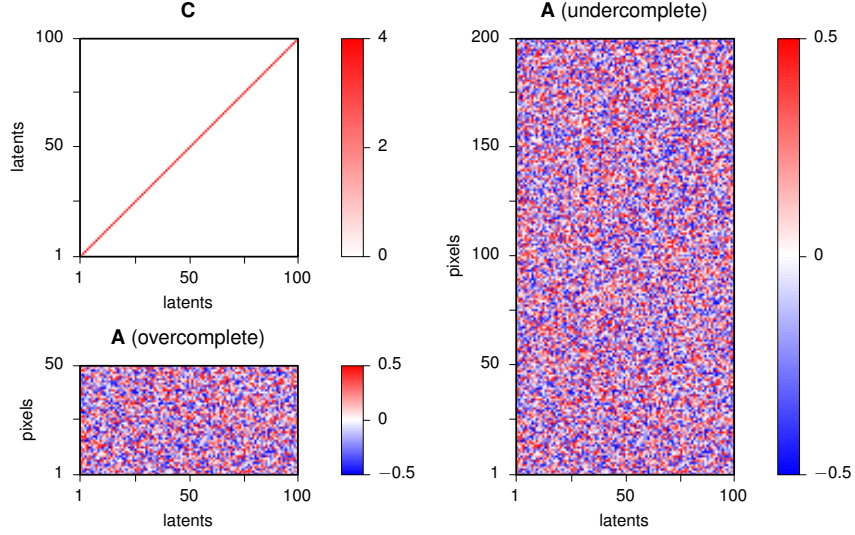


Figure 1. Identity prior covariance matrix \mathbf{C} (top left) together with random filter matrices \mathbf{A} used for numerical testing of the low and high contrast approximations in the overcomplete (bottom left) and undercomplete cases (right). Note that the over- and undercomplete cases only differed in the number of observations (rows) but not of the latent variables (columns) so that the same prior could be applied.

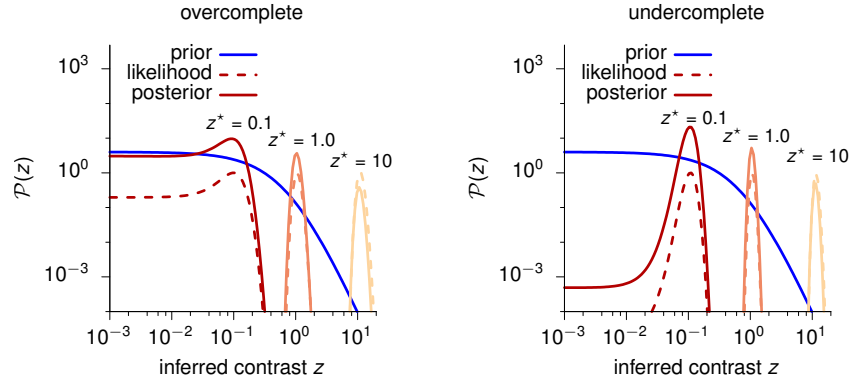


Figure 2. Prior distribution over z (blue), together with a few examples for the likelihood (shades of red, dashed) and posterior at different true contrast levels, z^* (shades of red, solid), in the overcomplete (left) and undercomplete case (right).

3.4 Numerical validation

In order to test the quality of our approximations in [Equations 14-17](#), we evaluated them together with the full expressions from [Equations 4-7](#) on a toy example. We chose an identity prior covariance \mathbf{C} (scaled by 4), a random filter matrix \mathbf{A} (each element sampled i.i.d. from a uniform between -0.5 and 0.5), and fixed the observation noise level to $\sigma_x^2 = 1$ ([Figure 1](#)). We generated the input image, \mathbf{x} , by sampling from the GSM ([Equations 1-2](#)) with the parameters described above and $z = z^*$, which we varied systematically⁴. (Specifically, to better isolate the effects of changing contrast, we used the same $\bar{\mathbf{x}}$ and frozen observation noise in [Equation 1](#) for generating \mathbf{x} at all values of z^*). To infer z , we used a power-law prior with $n = 4$ (such that both its mean and variance were finite) and $b = 0.75$. With these settings of the parameters, the posterior over z was mostly dominated by the likelihood

³A third case (not studied here) is possible, in which $\text{rank}(\mathbf{A}_o) < \min(N_{y_o}, N_x)$ (see [Appendix D](#)).

⁴This is slightly inconsistent with the simple scaling of input with z^* that we assumed for the derivations, [Equation 8](#) (see also [Footnote 2](#)), but consistent with the generative model of the GSM and thus ensures e.g. that inferences about z are well calibrated wrt. z^* .

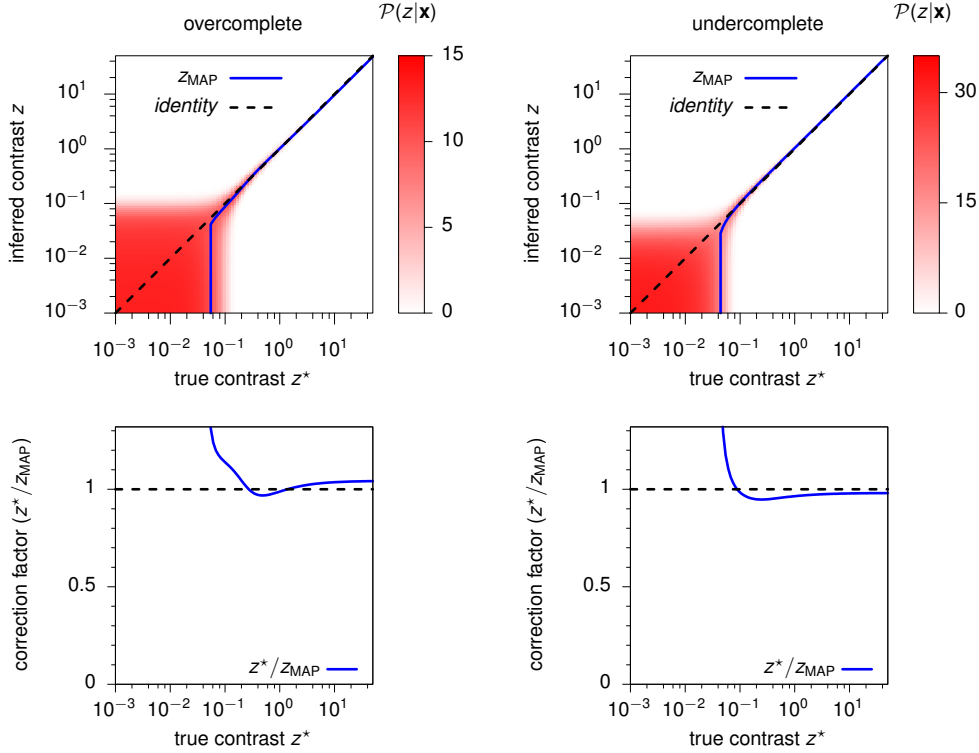


Figure 3. Top: posterior probability (color coded) of inferred contrast z given an image, \mathbf{x} , generated with true contrast z^* (see text for details); the value of z_{MAP} as a function of z^* is superimposed (blue lines). **Bottom:** correction factors z^*/z_{MAP} as a function of z^* , with dashed lines showing $z_{\text{MAP}} = z^*$. **Left:** overcomplete case. **Right:** undercomplete case.

(Figure 2). In particular, it was unimodal and tight, with z_{MAP} following z^* closely for all but the smallest true contrast levels (Figure 3). The z -likelihood – and thus the z -posterior – was even tighter in the undercomplete case as it involved a higher number of observed variables (Figure 1).

In order to explore the contrast-dependence of the mean and variance of the \mathbf{y} -posterior, we included a single element in \mathbf{y}_\bullet so that the corresponding mean and variance were scalars. Overall, we found that our approximations for both the low- and high-contrast limits were in good agreement with the full inference. In particular, they captured the qualitative dependence of both the mean and variance on contrast, as well as the way the mean and variance co-varied across different contrast levels (see Figures 4 and 5 for the over- and undercomplete cases, respectively).

We distinguished between two levels of approximation (see Section 3.1): one in which we took $\mathcal{P}(\mathbf{y}|\mathbf{x}) \simeq \mathcal{P}(\mathbf{y}|\mathbf{x}, z = z_{\text{MAP}})$ with z_{MAP} found via numerical optimization (Figures 4 and 5, panels A-C), and another one in which we assumed $z_{\text{MAP}} \simeq z^*$, leading to $\mathcal{P}(\mathbf{y}|\mathbf{x}) \simeq \mathcal{P}(\mathbf{y}|\mathbf{x}, z = z^*)$ (Figures 4 and 5, panels D-F). This second approximation had a more severe effect on the mean than on the variance, as the posterior variance under the GSM is independent of the true contrast, while z^* enters the equations of the mean via \mathbf{x} (compare Equations 5 and 6). Thus, the asymptotic behavior of the mean in the second approximation was consistently off from that of the first approximation by the ‘correction’ factor z^*/z_{MAP} (Figure 3, bottom; cf. Equations 48 and 49, Equations 68 and 69 and Equations 88 and 89 in Section 5). In particular, at low true contrasts, \mathbf{x} was dominated by the observation noise, so the z -posterior was dominated by the prior which had a peak at 0, resulting in $z_{\text{MAP}} = 0$ for a finite range of true contrasts (Figure 3, top). Consequently, the correction factor z^*/z_{MAP} diverged in the limit of small z^* (Figure 3, bottom). However, the assumption that the z -posterior is concentrated around z_{MAP} also broke down at low contrasts as it had considerable probability mass beyond z_{MAP} (Figure 3, top) and so the full \mathbf{y} -posterior behaved as if it was conditioned on a higher effective value of z than

without $z_{\text{MAP}} = z^*$ approximation

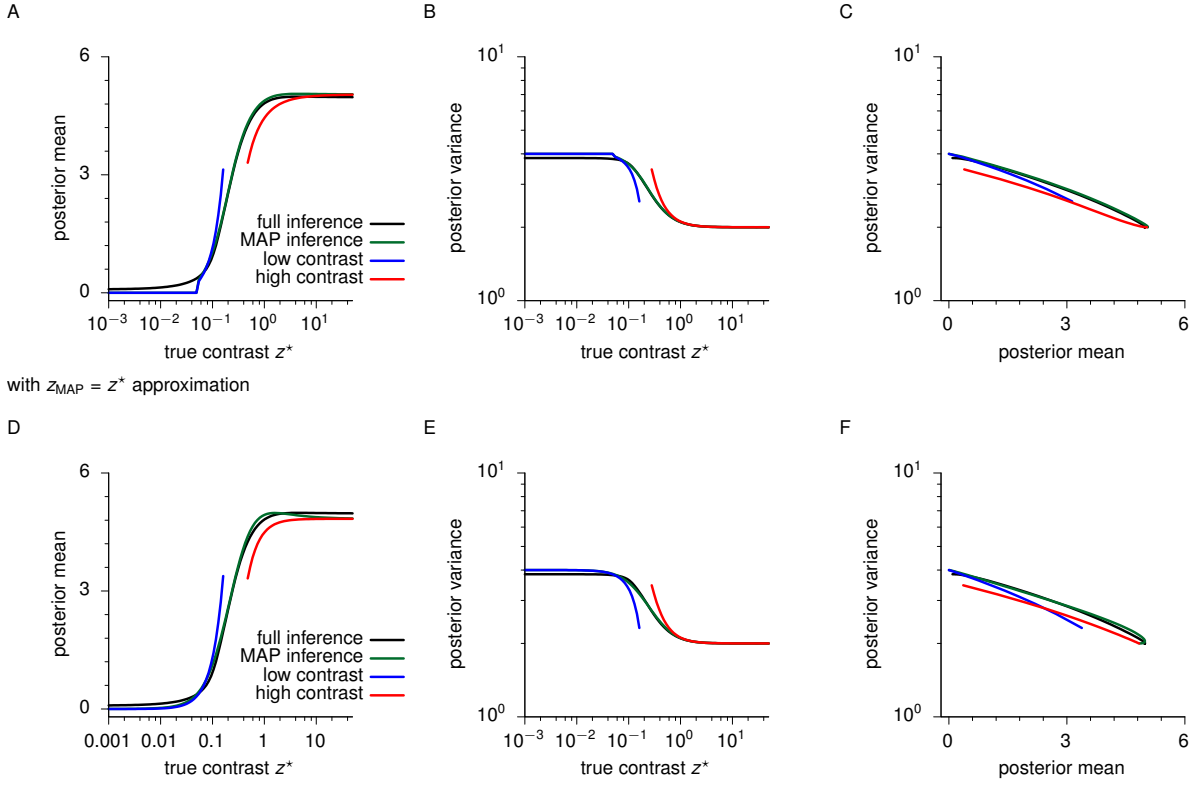
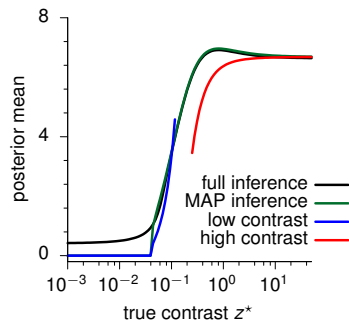


Figure 4. Dependence of posterior mean and variance on contrast in the overcomplete case. A-B, D-E: posterior mean (A, D) and variance (B, E), as functions of the true contrast level z^* . C, F: Posterior variance against posterior mean as z^* is varied. All panels, black: results of ‘full’ inference (obtained by numerically marginalising out the full z -posterior, [Equations 4-7](#)); green: MAP inference (by conditioning on $z = z_{\text{MAP}}$ in [Equations 5-6](#)); blue and red: low- and high-contrast approximations ([Equations 14-17](#)), respectively. Top panels (A, B, C): approximations using true z_{MAP} ; bottom panels (D, E, F): approximations substituting z_{MAP} with z^* .

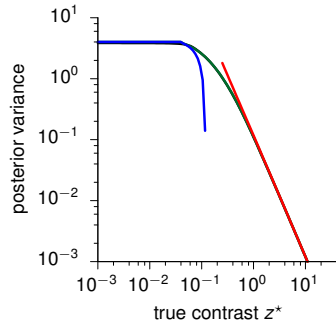
z_{MAP} (e.g. its mean did not converge to 0, and its variance did not converge to the prior variance as our analysis would have predicted). This meant that the second, seemingly more severe approximation, conditioning on z^* , which was consistently greater than z_{MAP} in this regime ([Figure 3](#), bottom), could in fact work better than the first one, conditioning on z_{MAP} (though it could still not predict the slightly above-zero mean at zero contrast). More generally, we found that neither approximation introduce significant errors by itself, and that they have a particularly negligible effect in the range $0.1 \leq z^* \leq 1.0$ over which the posterior mean and variance undergo most of their changes ([Figures 4 and 5](#), black vs. green).

without $z_{\text{MAP}} = z^*$ approximation

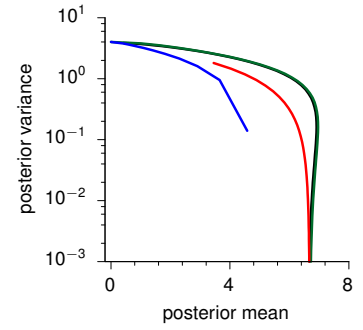
A



B

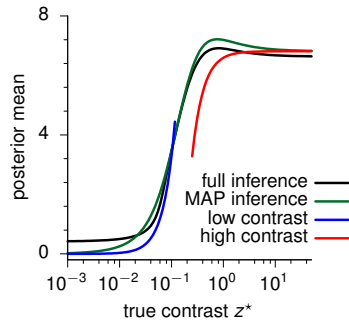


C

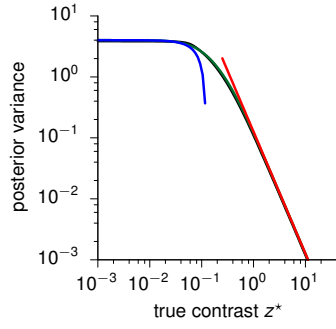


with $z_{\text{MAP}} = z^*$ approximation

D



E



F

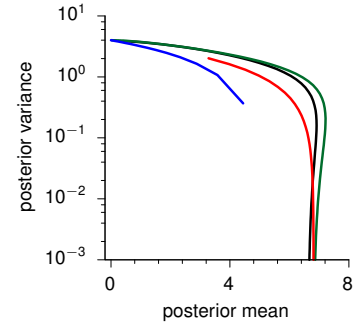


Figure 5. Same as Figure 4, for the undercomplete case.

4 Discussion

By using simple approximations, we were able to study analytically the dependence of the posterior mean and variance in the GSM in the limit of low and high contrast. In both limits, we found they converge quadratically with contrast to their respective limiting values. Our numerical results show that the approximations are valid within a reasonable range, indeed providing practical validity.

The characterization of the scaling of the mean and variance predicted by the GSM is highly relevant if it is to be applied to modeling neural data. While bottom up descriptions of neural dynamics, such as that provided by stabilized supralinear networks (Hennequin et al., 2016), predict a dependence of the statistical moments of neural activity similar to that of the features in the GSM, the precise scaling each model predicts for the moments of the posterior distribution may not be identical. We have shown here how the GSM is a suitable candidate to model neural data in which both mean and variance saturate in the limits of low and high contrasts, and they do so in an approximately quadratic way.

5 Methods

In the following we present the derivations for the scaling of the mean and variance in the limits of low and high contrast.

Low contrast limit, $z \rightarrow 0$

$$\lim_{z \rightarrow 0} \Sigma_{\bullet} = \left[\mathbf{C}_{\bullet}^{-1} + \frac{z^2}{\sigma_x^2} \bar{\mathbf{A}}_{\bullet}^{\top} \left(\frac{z^2}{\sigma_x^2} \bar{\mathbf{R}}_o + \mathbf{I} \right)^{-1} \bar{\mathbf{A}}_{\bullet} \right]^{-1} \quad (35)$$

$$\simeq \left[\mathbf{C}_{\bullet}^{-1} + \frac{z^2}{\sigma_x^2} \bar{\mathbf{A}}_{\bullet}^{\top} \left(\mathbf{I} - \frac{z^2}{\sigma_x^2} \bar{\mathbf{R}}_o \right) \bar{\mathbf{A}}_{\bullet} \right]^{-1} \quad (36)$$

$$\simeq \left[\mathbf{C}_{\bullet}^{-1} + \frac{z^2}{\sigma_x^2} \bar{\mathbf{A}}_{\bullet}^{\top} \bar{\mathbf{A}}_{\bullet} \right]^{-1} \quad (37)$$

$$\simeq \mathbf{C}_{\bullet} - \frac{z^2}{\sigma_x^2} \mathbf{C}_{\bullet} \bar{\mathbf{A}}_{\bullet}^{\top} \bar{\mathbf{A}}_{\bullet} \mathbf{C}_{\bullet} \quad (38)$$

$$= \Sigma_{\bullet}^0 - \frac{z^2}{\sigma_x^2} \mathbf{V}^{LC} \quad (39)$$

$$\simeq \Sigma_{\bullet}^0 - \frac{z^{*2}}{\sigma_x^2} \mathbf{V}^{LC} \quad (40)$$

with

$$\Sigma_{\bullet}^0 = \mathbf{C}_{\bullet} \quad (41)$$

$$\mathbf{V}^{LC} = \mathbf{C}_{\bullet} \bar{\mathbf{A}}_{\bullet}^{\top} \bar{\mathbf{A}}_{\bullet} \mathbf{C}_{\bullet} \quad (42)$$

$$\lim_{z \rightarrow 0} \mu_{\bullet} = \frac{z}{\sigma_x^2} \Sigma_{\bullet} \bar{\mathbf{A}}_{\bullet}^{\top} \left(\frac{z^2}{\sigma_x^2} \bar{\mathbf{R}}_o + \mathbf{I} \right)^{-1} \mathbf{x} \quad (43)$$

$$\simeq \frac{z}{\sigma_x^2} \Sigma_{\bullet} \bar{\mathbf{A}}_{\bullet}^{\top} \left(\mathbf{I} - \frac{z^2}{\sigma_x^2} \bar{\mathbf{R}}_o \right) \mathbf{x} \quad (44)$$

$$\simeq \frac{z}{\sigma_x^2} \Sigma_{\bullet} \bar{\mathbf{A}}_{\bullet}^{\top} \mathbf{x} \quad (45)$$

$$\simeq \frac{z}{\sigma_x^2} \mathbf{C}_{\bullet} \bar{\mathbf{A}}_{\bullet}^{\top} \mathbf{x} \quad (46)$$

$$= \frac{z z^{\star}}{\sigma_x^2} \mathbf{C}_{\bullet} \bar{\mathbf{A}}_{\bullet}^{\top} \bar{\mathbf{x}} \quad (47)$$

$$= \frac{z^{\star}}{z} \left(\mu_{\bullet}^0 + \frac{z^2}{\sigma_x^2} \mathbf{M}^{LC} \bar{\mathbf{x}} \right) \quad (48)$$

$$\simeq \mu_{\bullet}^0 + \frac{z^{\star 2}}{\sigma_x^2} \mathbf{M}^{LC} \bar{\mathbf{x}} \quad (49)$$

with

$$\mu_{\bullet}^0 = \mathbf{0} \quad (50)$$

$$\mathbf{M}^{LC} = \mathbf{C}_{\bullet} \bar{\mathbf{A}}_{\bullet}^{\top} \quad (51)$$

High contrast limit, $z \rightarrow \infty$

Overcomplete system ($\bar{\mathbf{R}}_o$ invertible)

$$\lim_{z \rightarrow \infty} \Sigma_{\bullet} = \left[\mathbf{C}_{\bullet}^{-1} + \frac{z^2}{\sigma_x^2} \bar{\mathbf{A}}_{\bullet}^{\top} \left(\frac{z^2}{\sigma_x^2} \bar{\mathbf{R}}_o + \mathbf{I} \right)^{-1} \bar{\mathbf{A}}_{\bullet} \right]^{-1} \quad (52)$$

$$= \left[\mathbf{C}_{\bullet}^{-1} + \bar{\mathbf{A}}_{\bullet}^{\top} \left(\bar{\mathbf{R}}_o + \frac{\sigma_x^2}{z^2} \mathbf{I} \right)^{-1} \bar{\mathbf{A}}_{\bullet} \right]^{-1} \quad (53)$$

$$\simeq \left[\mathbf{C}_{\bullet}^{-1} + \bar{\mathbf{A}}_{\bullet}^{\top} \left(\bar{\mathbf{R}}_o^{-1} - \frac{\sigma_x^2}{z^2} \bar{\mathbf{R}}_o^{-1} \bar{\mathbf{R}}_o^{-1} \right) \bar{\mathbf{A}}_{\bullet} \right]^{-1} \quad (54)$$

$$= \left[\mathbf{C}_{\bullet}^{-1} + \bar{\mathbf{A}}_{\bullet}^{\top} \bar{\mathbf{R}}_o^{-1} \bar{\mathbf{A}}_{\bullet} - \frac{\sigma_x^2}{z^2} \bar{\mathbf{A}}_{\bullet}^{\top} \bar{\mathbf{R}}_o^{-1} \bar{\mathbf{R}}_o^{-1} \bar{\mathbf{A}}_{\bullet} \right]^{-1} \quad (55)$$

$$\simeq \left(\mathbf{C}_{\bullet}^{-1} + \bar{\mathbf{A}}_{\bullet}^{\top} \bar{\mathbf{R}}_o^{-1} \bar{\mathbf{A}}_{\bullet} \right)^{-1} + \frac{\sigma_x^2}{z^2} \Sigma_{\bullet}^{\infty} \bar{\mathbf{A}}_{\bullet}^{\top} \bar{\mathbf{R}}_o^{-1} \bar{\mathbf{R}}_o^{-1} \bar{\mathbf{A}}_{\bullet} \Sigma_{\bullet}^{\infty} \quad (56)$$

$$= \Sigma_{\bullet}^{\infty} + \frac{\sigma_x^2}{z^2} \mathbf{V}^{HC} \quad (57)$$

$$\simeq \Sigma_{\bullet}^{\infty} + \frac{\sigma_x^2}{z^{\star 2}} \mathbf{V}^{HC} \quad (58)$$

with

$$\Sigma_{\bullet}^{\infty} = \left(\mathbf{C}_{\bullet}^{-1} + \bar{\mathbf{A}}_{\bullet}^{\top} \bar{\mathbf{R}}_o^{-1} \bar{\mathbf{A}}_{\bullet} \right)^{-1} \quad (59)$$

$$\mathbf{V}^{HC} = \Sigma_{\bullet}^{\infty} \bar{\mathbf{A}}_{\bullet}^{\top} \bar{\mathbf{R}}_o^{-1} \bar{\mathbf{R}}_o^{-1} \bar{\mathbf{A}}_{\bullet} \Sigma_{\bullet}^{\infty} \quad (60)$$

$$\lim_{z \rightarrow \infty} \mu_{\bullet} = \frac{z}{\sigma_x^2} \Sigma_{\bullet} \bar{\mathbf{A}}_{\bullet}^T \left(\frac{z^2}{\sigma_x^2} \bar{\mathbf{R}}_o + \mathbf{I} \right)^{-1} \mathbf{x} \quad (61)$$

$$= \frac{\sigma_x^2}{z^2} \frac{z}{\sigma_x^2} \Sigma_{\bullet} \bar{\mathbf{A}}_{\bullet}^T \left(\bar{\mathbf{R}}_o + \frac{\sigma_x^2}{z^2} \mathbf{I} \right)^{-1} \mathbf{x} \quad (62)$$

$$\simeq \frac{1}{z} \Sigma_{\bullet} \bar{\mathbf{A}}_{\bullet}^T \left(\bar{\mathbf{R}}_o^{-1} - \frac{\sigma_x^2}{z^2} \bar{\mathbf{R}}_o^{-1} \bar{\mathbf{R}}_o^{-1} \right) \mathbf{x} \quad (63)$$

$$\simeq \frac{1}{z} \left(\Sigma_{\bullet}^{\infty} + \frac{\sigma_x^2}{z^2} \Sigma_{\bullet}^{\infty} \bar{\mathbf{A}}_{\bullet}^T \bar{\mathbf{R}}_o^{-1} \bar{\mathbf{R}}_o^{-1} \bar{\mathbf{A}}_{\bullet} \Sigma_{\bullet}^{\infty} \right) \bar{\mathbf{A}}_{\bullet}^T \left(\bar{\mathbf{R}}_o^{-1} - \frac{\sigma_x^2}{z^2} \bar{\mathbf{R}}_o^{-1} \bar{\mathbf{R}}_o^{-1} \right) z^* \bar{\mathbf{x}} \quad (64)$$

$$= \frac{z^*}{z} \left(\Sigma_{\bullet}^{\infty} + \frac{\sigma_x^2}{z^2} \Sigma_{\bullet}^{\infty} \bar{\mathbf{A}}_{\bullet}^T \bar{\mathbf{R}}_o^{-1} \bar{\mathbf{R}}_o^{-1} \bar{\mathbf{A}}_{\bullet} \Sigma_{\bullet}^{\infty} \right) \bar{\mathbf{A}}_{\bullet}^T \left(\bar{\mathbf{R}}_o^{-1} - \frac{\sigma_x^2}{z^2} \bar{\mathbf{R}}_o^{-1} \bar{\mathbf{R}}_o^{-1} \right) \bar{\mathbf{x}} \quad (65)$$

$$\simeq \Sigma_{\bullet}^{\infty} \bar{\mathbf{A}}_{\bullet}^T \bar{\mathbf{R}}_o^{-1} \frac{z^*}{z} \bar{\mathbf{x}} - \frac{\sigma_x^2}{z^2} \left(\Sigma_{\bullet}^{\infty} \bar{\mathbf{A}}_{\bullet}^T \bar{\mathbf{R}}_o^{-1} \bar{\mathbf{R}}_o^{-1} - \Sigma_{\bullet}^{\infty} \bar{\mathbf{A}}_{\bullet}^T \bar{\mathbf{R}}_o^{-1} \bar{\mathbf{R}}_o^{-1} \bar{\mathbf{A}}_{\bullet} \Sigma_{\bullet}^{\infty} \bar{\mathbf{A}}_{\bullet}^T \bar{\mathbf{R}}_o^{-1} \right) \frac{z^*}{z} \bar{\mathbf{x}} \quad (66)$$

$$= \Sigma_{\bullet}^{\infty} \bar{\mathbf{A}}_{\bullet}^T \bar{\mathbf{R}}_o^{-1} \frac{z^*}{z} \bar{\mathbf{x}} - \frac{\sigma_x^2}{z^2} \Sigma_{\bullet}^{\infty} \bar{\mathbf{A}}_{\bullet}^T \bar{\mathbf{R}}_o^{-1} \bar{\mathbf{R}}_o^{-1} \left(\mathbf{I} - \bar{\mathbf{A}}_{\bullet} \Sigma_{\bullet}^{\infty} \bar{\mathbf{A}}_{\bullet}^T \bar{\mathbf{R}}_o^{-1} \right) \frac{z^*}{z} \bar{\mathbf{x}} \quad (67)$$

$$= \frac{z^*}{z} \left(\mu_{\bullet}^{\infty} - \frac{\sigma_x^2}{z^2} \mathbf{M}^{HC} \bar{\mathbf{x}} \right) \quad (68)$$

$$\simeq \mu_{\bullet}^{\infty} - \frac{\sigma_x^2}{z^{*2}} \mathbf{M}^{HC} \bar{\mathbf{x}} \quad (69)$$

with

$$\mu_{\bullet}^{\infty} = \Sigma_{\bullet}^{\infty} \bar{\mathbf{A}}_{\bullet}^T \bar{\mathbf{R}}_o^{-1} \bar{\mathbf{x}} \quad (70)$$

$$\mathbf{M}^{HC} = \Sigma_{\bullet}^{\infty} \bar{\mathbf{A}}_{\bullet}^T \bar{\mathbf{R}}_o^{-1} \bar{\mathbf{R}}_o^{-1} \left(\mathbf{I} - \bar{\mathbf{A}}_{\bullet} \Sigma_{\bullet}^{\infty} \bar{\mathbf{A}}_{\bullet}^T \bar{\mathbf{R}}_o^{-1} \right) \quad (71)$$

Undercomplete system ($\bar{\mathbf{R}}_o$ non-invertible)

Here, we will make use of [Equation 22](#) and note that if $\bar{\mathbf{R}}_o = \mathbf{A}_o \mathbf{L}_o \mathbf{L}_o^T \mathbf{A}_o^T$ is low-rank and thus non-invertible it is still possible for $\mathbf{L}_o^T \mathbf{A}_o^T \mathbf{A}_o \mathbf{L}_o$ to be full-rank and invertible (what we here call the undercomplete case), and so \mathbf{Q}_o is non-degenerate even in the $z \rightarrow \infty$ limit (see [Appendix B](#) for computing $\mathbf{Q}_o = \left(\frac{z^2}{\sigma_x^2} \bar{\mathbf{R}}_o + \mathbf{I} \right)^{-1}$ and its asymptotic form in this case).

$$\lim_{z \rightarrow \infty} \Sigma_{\bullet} = \left[\mathbf{C}_{\bullet}^{-1} + \frac{z^2}{\sigma_x^2} \bar{\mathbf{A}}_{\bullet}^{\top} \left(\frac{z^2}{\sigma_x^2} \bar{\mathbf{R}}_o + \mathbf{I} \right)^{-1} \bar{\mathbf{A}}_{\bullet} \right]^{-1} \quad (72)$$

$$= \left[\mathbf{C}_{\bullet}^{-1} + \frac{z^2}{\sigma_x^2} \bar{\mathbf{A}}_{\bullet}^{\top} \mathbf{Q}_o \bar{\mathbf{A}}_{\bullet} \right]^{-1} \quad (73)$$

$$\simeq \left[\mathbf{C}_{\bullet}^{-1} + \frac{z^2}{\sigma_x^2} \bar{\mathbf{A}}_{\bullet}^{\top} \left(\mathbf{Q}_o^{\infty} + \frac{\sigma_x^2}{z^2} \bar{\mathbf{Q}}_o \right) \bar{\mathbf{A}}_{\bullet} \right]^{-1} \quad (74)$$

$$= \left[\mathbf{C}_{\bullet}^{-1} + \bar{\mathbf{A}}_{\bullet}^{\top} \bar{\mathbf{Q}}_o \bar{\mathbf{A}}_{\bullet} + \frac{z^2}{\sigma_x^2} \bar{\mathbf{A}}_{\bullet}^{\top} \mathbf{Q}_o^{\infty} \bar{\mathbf{A}}_{\bullet} \right]^{-1} \quad (75)$$

$$\simeq \frac{\sigma_x^2}{z^{*2}} \mathbf{V}^{HC} \quad (76)$$

$$= \Sigma_{\bullet}^{\infty} + \frac{\sigma_x^2}{z^{*2}} \mathbf{V}^{HC} \quad (77)$$

with

$$\Sigma_{\bullet}^{\infty} = \mathbf{0} \quad (78)$$

$$\mathbf{V}^{HC} = \left(\bar{\mathbf{A}}_{\bullet}^{\top} \mathbf{Q}_o^{\infty} \bar{\mathbf{A}}_{\bullet} \right)^{-1} \quad (79)$$

$$\mathbf{Q}_o^{\infty} = \mathbf{I} - \mathbf{A}_o \mathbf{L}_o \left(\mathbf{L}_o^{\top} \mathbf{A}_o^{\top} \mathbf{A}_o \mathbf{L}_o \right)^{-1} \mathbf{L}_o^{\top} \mathbf{A}_o^{\top} \quad (80)$$

$$\bar{\mathbf{Q}}_o = \mathbf{A}_o \mathbf{L}_o \left(\mathbf{L}_o^{\top} \mathbf{A}_o^{\top} \mathbf{A}_o \mathbf{L}_o \right)^{-2} \mathbf{L}_o^{\top} \mathbf{A}_o^{\top} \quad (81)$$

As we shall see below, for deriving the asymptotic behaviour of μ_{\bullet} we will need Σ_{\bullet} up to higher order terms (as the $1/z^2$ term of Σ_{\bullet} will cancel), for which we need a bit of extra work restarting from [Equation 75](#):

$$\lim_{z \rightarrow \infty} \Sigma_{\bullet} \simeq \frac{\sigma_x^2}{z^2} \left[\frac{\sigma_x^2}{z^2} \left(\mathbf{C}_{\bullet}^{-1} + \bar{\mathbf{A}}_{\bullet}^{\top} \bar{\mathbf{Q}}_o \bar{\mathbf{A}}_{\bullet} \right) + \left(\mathbf{V}^{HC} \right)^{-1} \right]^{-1} \quad (82)$$

$$\simeq \frac{\sigma_x^2}{z^2} \left[\mathbf{V}^{HC} - \frac{\sigma_x^2}{z^2} \mathbf{V}^{HC} \left(\mathbf{C}_{\bullet}^{-1} + \bar{\mathbf{A}}_{\bullet}^{\top} \bar{\mathbf{Q}}_o \bar{\mathbf{A}}_{\bullet} \right) \mathbf{V}^{HC} \right] \quad (83)$$

Now we are in the position to look at the asymptotic behaviour of the posterior mean.

$$\lim_{z \rightarrow \infty} \mu_{\bullet} = \frac{z}{\sigma_x^2} \Sigma_{\bullet} \bar{\mathbf{A}}_{\bullet}^{\top} \left(\frac{z^2}{\sigma_x^2} \bar{\mathbf{R}}_o + \mathbf{I} \right)^{-1} \mathbf{x} \quad (84)$$

$$= \frac{z z^*}{\sigma_x^2} \Sigma_{\bullet} \bar{\mathbf{A}}_{\bullet}^{\top} \mathbf{Q}_o \bar{\mathbf{x}} \quad (85)$$

$$\simeq \frac{z z^*}{\sigma_x^2} \frac{\sigma_x^2}{z^2} \left[\mathbf{V}^{HC} - \frac{\sigma_x^2}{z^2} \mathbf{V}^{HC} \left(\mathbf{C}_{\bullet}^{-1} + \bar{\mathbf{A}}_{\bullet}^{\top} \bar{\mathbf{Q}}_o \bar{\mathbf{A}}_{\bullet} \right) \mathbf{V}^{HC} \right] \bar{\mathbf{A}}_{\bullet}^{\top} \left(\mathbf{Q}_o^{\infty} + \frac{\sigma_x^2}{z^2} \bar{\mathbf{Q}}_o \right) \bar{\mathbf{x}} \quad (86)$$

$$= \mathbf{V}^{HC} \bar{\mathbf{A}}_{\bullet}^{\top} \mathbf{Q}_o^{\infty} \frac{z^*}{z} \bar{\mathbf{x}} - \frac{\sigma_x^2}{z^2} \mathbf{V}^{HC} \left[\left(\mathbf{C}_{\bullet}^{-1} + \bar{\mathbf{A}}_{\bullet}^{\top} \bar{\mathbf{Q}}_o \bar{\mathbf{A}}_{\bullet} \right) \mathbf{V}^{HC} \bar{\mathbf{A}}_{\bullet}^{\top} \mathbf{Q}_o^{\infty} - \bar{\mathbf{A}}_{\bullet}^{\top} \bar{\mathbf{Q}}_o \right] \frac{z^*}{z} \bar{\mathbf{x}} \quad (87)$$

$$= \frac{z^*}{z} \left(\mu_{\bullet}^{\infty} - \frac{\sigma_x^2}{z^2} \mathbf{M}^{HC} \bar{\mathbf{x}} \right) \quad (88)$$

$$\simeq \mu_{\bullet}^{\infty} - \frac{\sigma_x^2}{z^{*2}} \mathbf{M}^{HC} \bar{\mathbf{x}} \quad (89)$$

where

$$\mu_{\bullet}^{\infty} = \mathbf{V}^{HC} \bar{\mathbf{A}}_{\bullet}^{\top} \mathbf{Q}_o^{\infty} \bar{\mathbf{x}} \quad (90)$$

$$\mathbf{M}^{HC} = \mathbf{V}^{HC} \left[\left(\mathbf{C}_{\bullet}^{-1} + \bar{\mathbf{A}}_{\bullet}^{\top} \bar{\mathbf{Q}}_o \bar{\mathbf{A}}_{\bullet} \right) \mathbf{V}^{HC} \bar{\mathbf{A}}_{\bullet}^{\top} \mathbf{Q}_o^{\infty} - \bar{\mathbf{A}}_{\bullet}^{\top} \bar{\mathbf{Q}}_o \right] \quad (91)$$

References

- Coen-Cagli, R., Kohn, A., and Schwartz, O. (2015). Flexible gating of contextual influences in natural vision. *Nature neuroscience*.
- Fiser, J., Berkes, B., Orbán, G., and Lengyel, M. (2010). Statistically optimal perception and learning: from behavior to neural representations. *Trends Cogn Sci*, 14:119–30.
- Hennequin, G., Ahmadian, Y., Rubin, D. B., Lengyel, M., and Miller, K. D. (2016). Stabilized supralinear network dynamics account for stimulus-induced changes of noise variability in the cortex. *bioRxiv*, page 094334.
- Orbán, G., Berkes, P., Fiser, J., and Lengyel, M. (2016). Neural variability and sampling-based probabilistic representations in the visual cortex. *Neuron*, 92(2):530–543.
- Schwartz, O. and Simoncelli, E. P. (2001). Natural signal statistics and sensory gain control. *Nature neuroscience*, 4(8):819–825.
- Wainwright, M. J. and Simoncelli, E. P. (1999). Scale mixtures of gaussians and the statistics of natural images. In *Nips*, pages 855–861.

Appendix

A Deriving the low-dimensional posterior

The first step is to write the predictive distribution in terms of \mathbf{y}_\bullet (marginalising out \mathbf{y}_\circ). This is easiest to do by rewriting [Equation 1](#) as

$$\mathbf{x} = z \mathbf{A} \mathbf{y} + \sigma_x^2 \epsilon \quad \epsilon \sim \mathcal{N}(\mathbf{0}, \mathbf{I}) \quad (92)$$

$$= z \mathbf{A}_\bullet \mathbf{y}_\bullet + z \mathbf{A}_\circ \mathbf{y}_\circ + \sigma_x^2 \epsilon \quad (93)$$

importantly, here we treat \mathbf{y}_\circ just as much as a random variable as ϵ , and its distribution *conditioned on* \mathbf{y}_\bullet has the following mean and covariance (knowing that the prior mean of both \mathbf{y}_\bullet and \mathbf{y}_\circ is $\mathbf{0}$):

$$\mathbb{E}[\mathbf{y}_\circ | \mathbf{y}_\bullet] = \mathbf{C}_{\circ\bullet} \mathbf{C}_\bullet^{-1} \mathbf{y}_\bullet \quad (94)$$

$$\text{Cov}[\mathbf{y}_\circ | \mathbf{y}_\bullet] = \mathbf{C}_\circ - \mathbf{C}_{\circ\bullet} \mathbf{C}_\bullet^{-1} \mathbf{C}_{\circ\bullet}^\top \quad (95)$$

As all our component distributions are normal, from this it follows that

$$\mathbf{x} | \mathbf{y}_\bullet, z \sim \mathcal{N}(z \bar{\mathbf{A}}_\bullet \mathbf{y}_\bullet, z^2 \bar{\mathbf{R}}_\circ + \sigma_x^2 \mathbf{I}) \quad (96)$$

where

$$\bar{\mathbf{A}}_\bullet = \mathbf{A}_\bullet + \mathbf{A}_\circ \mathbf{C}_{\circ\bullet} \mathbf{C}_\bullet^{-1} \quad (97)$$

$$\bar{\mathbf{R}}_\circ = \mathbf{A}_\circ (\mathbf{C}_\circ - \mathbf{C}_{\circ\bullet} \mathbf{C}_\bullet^{-1} \mathbf{C}_{\circ\bullet}^\top) \mathbf{A}_\circ^\top \quad (98)$$

Next, we rewrite the predictive distribution as an (unnormalised) distribution over \mathbf{y}_\bullet :

$$\begin{aligned} \mathcal{N}(\mathbf{x}; z \bar{\mathbf{A}}_\bullet \mathbf{y}_\bullet, z^2 \bar{\mathbf{R}}_\circ + \sigma_x^2 \mathbf{I}) \\ = \mathcal{N}(z \bar{\mathbf{A}}_\bullet \mathbf{y}_\bullet; \mathbf{x}, z^2 \bar{\mathbf{R}}_\circ + \sigma_x^2 \mathbf{I}) \end{aligned} \quad (99)$$

$$\propto \mathcal{N}(\mathbf{y}_\bullet; \mathbf{m}_\bullet, \mathbf{S}_\bullet) \quad (100)$$

$$\mathbf{m}_\bullet = \frac{z}{\sigma_x^2} \mathbf{S}_\bullet \bar{\mathbf{A}}_\bullet^\top \left(\frac{z^2}{\sigma_x^2} \bar{\mathbf{R}}_\circ + \mathbf{I} \right)^{-1} \mathbf{x} \quad (101)$$

$$\mathbf{S}_\bullet^{-1} = \frac{z^2}{\sigma_x^2} \bar{\mathbf{A}}_\bullet^\top \left(\frac{z^2}{\sigma_x^2} \bar{\mathbf{R}}_\circ + \mathbf{I} \right)^{-1} \bar{\mathbf{A}}_\bullet \quad (102)$$

This allows us to derive the low-dimensional posterior as (c.f. [Equations 9-11](#))

$$\mathbf{y}_\bullet | \mathbf{x}, z \sim \mathcal{N}(\boldsymbol{\mu}_\bullet, \boldsymbol{\Sigma}_\bullet) \quad (103)$$

$$\text{where } \boldsymbol{\mu}_\bullet = \frac{z}{\sigma_x^2} \boldsymbol{\Sigma}_\bullet \bar{\mathbf{A}}_\bullet^\top \left(\frac{z^2}{\sigma_x^2} \bar{\mathbf{R}}_\circ + \mathbf{I} \right)^{-1} \mathbf{x} \quad (104)$$

$$\text{and } \boldsymbol{\Sigma}_\bullet = \left[\mathbf{C}_\bullet^{-1} + \frac{z^2}{\sigma_x^2} \bar{\mathbf{A}}_\bullet^\top \left(\frac{z^2}{\sigma_x^2} \bar{\mathbf{R}}_\circ + \mathbf{I} \right)^{-1} \bar{\mathbf{A}}_\bullet \right]^{-1} \quad (105)$$

B Computing the inverse of $\left(\frac{z^2}{\sigma_x^2} \bar{\mathbf{R}}_\circ + \mathbf{I} \right)$ and its asymptotic form in the undercomplete case

This is relevant for computing both the posterior mean ([Equation 10](#)) and covariance ([Equation 11](#)). By making use of the Cholesky decomposition of $\bar{\mathbf{R}}_\circ$ in [Equation 22](#) and the Woodbury identity, we

obtain:

$$\mathbf{Q}_o = \left(\frac{z^2}{\sigma_x^2} \bar{\mathbf{R}}_o + \mathbf{I} \right)^{-1} \quad (106)$$

$$= \left(\frac{z^2}{\sigma_x^2} \mathbf{A}_o \mathbf{L}_o \mathbf{L}_o^T \mathbf{A}_o^T + \mathbf{I} \right)^{-1} \quad (107)$$

$$= \mathbf{I} - \frac{z^2}{\sigma_x^2} \mathbf{A}_o \mathbf{L}_o \left(\frac{z^2}{\sigma_x^2} \mathbf{L}_o^T \mathbf{A}_o^T \mathbf{A}_o \mathbf{L}_o + \mathbf{I} \right)^{-1} \mathbf{L}_o^T \mathbf{A}_o^T \quad (108)$$

$$= \mathbf{I} - \mathbf{A}_o \mathbf{L}_o \left(\mathbf{L}_o^T \mathbf{A}_o^T \mathbf{A}_o \mathbf{L}_o + \frac{\sigma_x^2}{z^2} \mathbf{I} \right)^{-1} \mathbf{L}_o^T \mathbf{A}_o^T \quad (109)$$

We will be particularly interested in the asymptotic form of \mathbf{Q}_o , which can be written as:

$$\lim_{z \rightarrow \infty} \mathbf{Q}_o \simeq \mathbf{I} - \mathbf{A}_o \mathbf{L}_o \left[\left(\mathbf{L}_o^T \mathbf{A}_o^T \mathbf{A}_o \mathbf{L}_o \right)^{-1} - \frac{\sigma_x^2}{z^2} \left(\mathbf{L}_o^T \mathbf{A}_o^T \mathbf{A}_o \mathbf{L}_o \right)^{-2} \right] \mathbf{L}_o^T \mathbf{A}_o^T \quad (110)$$

$$= \mathbf{Q}_o^\infty + \frac{\sigma_x^2}{z^2} \bar{\mathbf{Q}}_o \quad (111)$$

$$\text{with } \mathbf{Q}_o^\infty = \mathbf{I} - \mathbf{A}_o \mathbf{L}_o \left(\mathbf{L}_o^T \mathbf{A}_o^T \mathbf{A}_o \mathbf{L}_o \right)^{-1} \mathbf{L}_o^T \mathbf{A}_o^T \quad (112)$$

$$\bar{\mathbf{Q}}_o = \mathbf{A}_o \mathbf{L}_o \left(\mathbf{L}_o^T \mathbf{A}_o^T \mathbf{A}_o \mathbf{L}_o \right)^{-2} \mathbf{L}_o^T \mathbf{A}_o^T \quad (113)$$

We note that when $\bar{\mathbf{R}}_o = \mathbf{A}_o \mathbf{L}_o \mathbf{L}_o^T \mathbf{A}_o^T$ is low-rank and thus non-invertible, it is still possible for $\mathbf{L}_o^T \mathbf{A}_o^T \mathbf{A}_o \mathbf{L}_o$ to be full-rank and invertible (what we have here denoted the undercomplete case), and so \mathbf{Q}_o is non-degenerate even in the $z \rightarrow \infty$ limit.

C Numerical evaluation of z_{MAP}

We have considered in the present work two approaches to find the numerical value of z_{MAP} , without substantial differences between them.

The first possibility is to perform a grid-search over $\mathcal{P}(z|\mathbf{x}) \propto \mathcal{P}(\mathbf{x}|z) \mathcal{P}(z)$, since we already have these values as computed for the colormap of [Figure 3](#). The drawback is that one needs to ensure to have a fine enough mesh around the peak value (of which one does not know the location *a priori*) to find a reasonable value of z_{MAP} .

An alternative is then to find the value of z for which the first derivative of the posterior (or, for practicality, the log-posterior) vanishes, that is:

$$\frac{\partial}{\partial z} \log \mathcal{P}(z|\mathbf{x}) = \frac{\partial}{\partial z} \log \mathcal{P}(z) + \frac{\partial}{\partial z} \log \mathcal{P}(\mathbf{x}|z) \quad (114)$$

We have:

$$\log \mathcal{P}(z) = -n \log(z + b) + ctt. \quad (115)$$

$$\frac{\partial}{\partial z} \log \mathcal{P}(z) = -\frac{n}{z + b} \quad (116)$$

and

$$\log \mathcal{P}(\mathbf{x}|z) = -\frac{1}{2} \log |\mathbf{S}(z)| - \frac{1}{2} \mathbf{x}^T \mathbf{S}^{-1}(z) \mathbf{x} + ctt. \quad (117)$$

$$\frac{\partial}{\partial z} \log \mathcal{P}(\mathbf{x}|z) = -z \operatorname{Tr} [\mathbf{S}^{-1} (\mathbf{I} - \mathbf{x} \mathbf{x}^T \mathbf{S}^{-1}(z)) \mathbf{A} \mathbf{C} \mathbf{A}^T] \quad (118)$$

with

$$\mathbf{S} = \sigma_x^2 \mathbf{I} + z^2 \mathbf{A} \mathbf{C} \mathbf{A}^T \quad (119)$$

Therefore, we look for the solution to the following 1D problem:

$$\frac{\partial}{\partial z} \log \mathcal{P}(z|\mathbf{x}) = -\frac{n}{z + b} - z \operatorname{Tr} [\mathbf{S}^{-1} (\mathbf{I} - \mathbf{x} \mathbf{x}^T \mathbf{S}^{-1}(z)) \mathbf{A} \mathbf{C} \mathbf{A}^T] \stackrel{!}{=} 0 \quad (120)$$

This expression can then be fed into any root finding routine, to obtain a candidate z_{MAP} . Since the derivative is not necessarily a monotonic function, one finally needs to check that the root thus found is a local maximum and not a minimum and, if so, whether it is truly a global maximum, also comparing the posterior there with the posterior at the $z = 0$ boundary.

D On the invertibility of $\overline{\mathbf{R}}_o$ and its rank

We know that for any real matrix \mathbf{M} :

$$\operatorname{rank}(\mathbf{M} \mathbf{M}^T) = \operatorname{rank}(\mathbf{M}^T \mathbf{M}) = \operatorname{rank}(\mathbf{M}) = \operatorname{rank}(\mathbf{M}^T) \quad (121)$$

In particular, if $\mathbf{M} = \mathbf{A}_o \mathbf{L}_o$, we see that:

$$\operatorname{rank}(\overline{\mathbf{R}}_o) = \operatorname{rank}(\mathbf{A}_o \mathbf{L}_o \mathbf{L}_o^T \mathbf{A}_o^T) = \operatorname{rank}(\mathbf{L}_o^T \mathbf{A}_o^T \mathbf{A}_o \mathbf{L}_o) = \operatorname{rank}(\mathbf{A}_o \mathbf{L}_o) \quad (122)$$

So if $\operatorname{rank}(\mathbf{A}_o \mathbf{L}_o) = r < \min(N_x, N_{y_o})$ where $\mathbf{A}_o \mathbf{L}_o \in \mathbb{R}^{N_x \times N_{y_o}}$, then both $\mathbf{A}_o \mathbf{L}_o \mathbf{L}_o^T \mathbf{A}_o^T$ and $\mathbf{L}_o^T \mathbf{A}_o^T \mathbf{A}_o \mathbf{L}_o$ will be low rank and therefore not invertible. If this is the case, we can use neither the overcomplete nor the undercomplete approximation here presented in the high contrast regime.